metals

MDPI

Article

Deformation Structure and Mechanical Properties of Pure Titanium Produced by Rotary-Die Equal-Channel Angular Pressing

Yanxia Gu [1,2], Aibin Ma [1,3,*], Jinghua Jiang [1,3], Yuchun Yuan [1] and Huiyun Li [1]

1 College of Mechanics and Materials, Hohai University, Nanjing 211100, China; guyanxiaj@126.com (Y.G.); jinghua-jiang@hhu.edu.cn (J.J.); yychehai@163.com (Y.Y.); lea_ori@163.com (H.L.)
2 Jiangsu Maritime Institute, Nanjing 211100, China
3 Suqian Institute, Hohai University, Suqian 223800, China
* Correspondence: aibin-ma@hhu.edu.cn; Tel.: +86-025-8378-7239

Received: 25 June 2017; Accepted: 30 July 2017; Published: 3 August 2017

Abstract: Pure titanium was efficiently processed up to four passes at 420 °C by rotary-die equal-channel angular pressing (RD-ECAP). The deformation structure and mechanical properties of pure titanium with various RD-ECAP passes were subsequently investigated. Microstructure evolution revealed that plastic deformation was accommodated mainly by twins during the first and second passes, while the predominant deformation mechanism was dislocation slip during the third and fourth passes. $\{10\bar{1}2\}$ twins were detected in the first pass, and $\{10\bar{1}1\}$ twins occurred in the second pass of RD-ECAP. The ultimate tensile strength of pure titanium increased from 450 MPa in the as-received state to 627 MPa with a fracture elongation of 29% after four passes of RD-ECAP.

Keywords: pure titanium; rotary-die equal-channel angular pressing (RD-ECAP); microstructure; mechanical properties; deformation

1. Introduction

The properties of metallic materials are closely related to the grain size. In partiular, the strength of materials increases with the reduction of grain diameter following the Hall-Petch rule, and this has given rise to an increasing interest in producing ultrafine-grained (UFG) materials with grains smaller than ~1 μm [1]. It has been reported that UFG materials exhibit superior properties, including high strength and good ductility, superplasticity, enhanced fatigue performance, improved conductivity, and so on [2]. Equal-channel angular pressing (ECAP) has received ever-rising attention and has now become a well-established and promising severe plastic deformation technique of producing UFG materials [3]. However, the conventional ECAP process is a labor-intensive and time-consuming procedure, as the sample needs to be taken out of the die and reinserted between each pass. It takes a long time to obtain a large number of passes and thus makes the conventional ECAP process inefficient for industrial application.

To solve the problem of low efficiency, several alternative procedures have been proposed. Nishida et al. [4] developed rotary-die ECAP (RD-ECAP), a procedure that effectively circumvents the limitation of the removing and re-inserting procedure. The billet can be continuously pressed by rotating the die during passes. Thus, multiple passes of ECAP can be rapidly and easily carried out on the samples without removing them from the die. RD-ECAP processing is categorized into route A in the conventional ECAP process, by which the sample is pressed without rotation between passes [4]. However, it should be noted that the front and rear parts of samples were alternated in RD-ECAP, while the pressing direction was the same in the conventional ECAP process by route A. That results in differences in deformation of billets through these two procedures. It is verified that the deformation

in the high-efficiency RD-ECAP is distinct from that in conventional route A both experimentally [5] and theoretically [6].

Titanium has received much interest recently because of its excellent biocompatibility and its potential as an implant material [7]. The widespread application of titanium requires an in-depth exploration of its deformation mechanism. The <a> slip systems in titanium include basal {0002}<11$\bar{2}$0>, prismatic {10$\bar{1}$0}<11$\bar{2}$0>, and pyramidal {10$\bar{1}$1}<11$\bar{2}$0> [8]. As <a> slips cannot provide enough independent slip systems to accommodate the imposed strain, <a + c> slips such as {10$\bar{1}$1}<11$\bar{2}$3> or twinning are usually activated [9,10]. There are several types of twins that have been found in titanium, including {10$\bar{1}$2}, {11$\bar{2}$1}, {11$\bar{2}$3} tensile twins, and {11$\bar{2}$2}, {10$\bar{1}$1}, {11$\bar{2}$4} compressive twins. The most frequently observed twinning modes in pure titanium during traditional deformation at room temperature are {10$\bar{1}$2} tensile twins and {11$\bar{2}$2} compressive twins [9–12]. {11$\bar{2}$1} tensile twins and {11$\bar{2}$4} compressive twins can be found in pure titanium subjected to dynamic plastic deformation (DPD) [13,14]; cryogenic channel-die compression [15]; high-speed compression [16], and other conditions [8,17]. In pure titanium subjected to ECAP, {10$\bar{1}$1} compressive twins became the primary twinning mode during the first pass at processing temperatures above 250 °C [18–20]. During ECAP processing at room temperature, the twinning modes of pure titanium for the first pass showed various situations. Zhao et al. [21] observed {10$\bar{1}$1} twins, while Zhang et al. [22] detected only {10$\bar{1}$2} twins in pure titanium after one pass of room-temperature ECAP deformation. Chen et al. [23] detected four types of twins including {10$\bar{1}$1}, {11$\bar{2}$1}, {10$\bar{1}$2}, and {11$\bar{2}$2} in pure Ti subjected to one pass of room-temperature ECAP. These results revealed that the activation of the twinning mode relies strongly on the angle between the loading direction and crystallographic orientation of the material, as well as the temperature, strain rate, and other deformation conditions. Although there have been considerable investigations on twinning modes during conventional ECAP, the microstructure evolution, deformation mechanism, and twinning sequences during RD-ECAP of pure titanium, in addition to the mechanical behavior after RD-ECAP, are still not well understood.

During ECAP, there are several parameters that influence the microstructure and mechanical properties of materials, including the geometrical parameter of the die, the pressing speed and temperature, the initial structure of materials, and so on. Previous studies showed that UFG Ti processed by ECAP exhibited improved mechanical properties. Moreover, the combination of both ECAP and thermal-mechanical treatment (TMT) such as rolling or drawing further enhanced the strength of commercially pure titanium (CP-Ti). An investigation by Stolyarov et al. [24] reported that the ultimate tensile strength of pure titanium (grade 2) increased from 487 MPa to 633 MPa after eight passes of ECAP, and further increased to 945 MPa by subsequent rolling. Valiev et al. [25] produced nanostructured CP-Ti by ECAP and TMT. The ECAP process was performed at 450 °C with four passes using a conventional ECAP die with a channel angle of 90°, and then the CP-Ti was subjected to forging and drawing with an accumulated deformation of 80%. The nanostructured CP-Ti provided superior mechanical and biomedical properties, and was demonstrated to be applicable for dental implants through clinic trails. However, the low efficiency of the conventional ECAP process is an obstacle for the large-scale industrial production of UFG Ti. It is obvious that there would be a significant raise in efficiency if the ECAP process of CP-Ti was carried out by RD-ECAP. In fact, to the authors' knowledge, the microstructure evolution and mechanical properties of pure titanium produced by RD-ECAP has not been studied to date. This paper provides information on the characterization of the deformation structure of CP-Ti during the process of RD-ECAP. The twinning modes were analyzed by transmission electron microscopy (TEM) and compared with other investigations. The mechanical properties of the material after RD-ECAP were also studied.

2. Materials and Methods

Commercially pure Ti (grade 2) was used in the present study. The chemical composition (wt %) of the samples was 0.015% C, 0.059% Fe, 0.062% O, 0.013% N, 0.002% H, and balance Ti. The as-received

raw material was in the form of hot-forged rods with diameters of 120 mm. The average grain size of the as-received samples was ~10 μm.

The initial titanium rods were cut into billets for RD-ECAP processing to be 40 mm in length and 19.5 × 19.5 mm^2 in cross-section. Figure 1 illustrates the diagrammatic drawing of RD-ECAP. The die is comprised by two perpendicular channels with equal cross-sections. The effective strain per pass in RD-ECAP is about 1.15. The inner diameter of the channel is 20 mm. The channel angle of the die is 90° and the curvature angle is zero. The die rests on the die holder, which contains a bottom plate and side plates. Three punches are inserted in the die in advance. They are marked as the bottom vertical punch, the right horizontal punch, and the left horizontal punch. The movement of the bottom vertical punch and right horizontal punch are confined by the bottom plate and the right plate, respectively. The billet is inserted in the die and the upper vertical punch is placed on the billet. Then the billet is pressed by the plunger through the left horizontal channel for the first pass. After that, the die is rotated clockwise by 90° and the rotation makes the press return to the initial state. Therefore, the subsequent passes can be performed continuously without removing the billet. Before processing, the billets, punches, and die were preheated to 420 °C. The billets were continuously pressed for one to four ECAP passes at the processing speed of 0.1 mm s^{-1}. The temperature dropped gradually to about 410 °C after each pass. Then, the billet and die were heated to 420 °C for 5 min for the next pass. Molybdenum disulphide and graphite were used as lubricants.

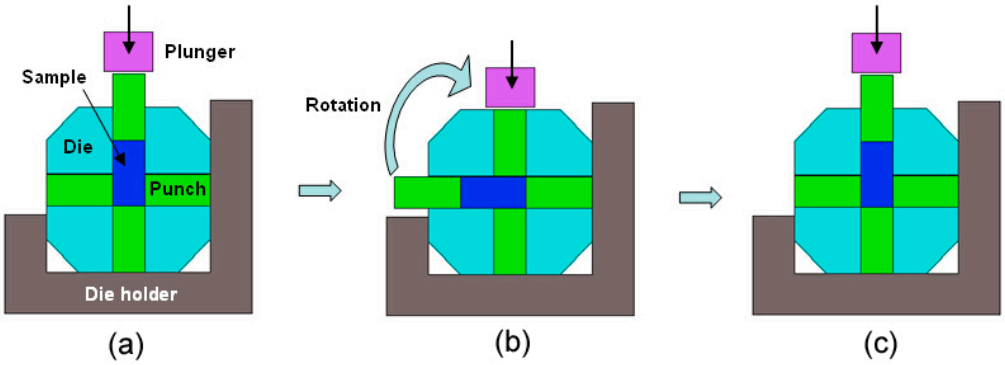

Figure 1. Diagrammatic drawing of RD-ECAP: (**a**) initial state; (**b**) rotation of the die; (**c**) after the rotation of the die.

The surfaces of the billets processed by ECAP were stripped by spark-cutting. All the specimens for microstructure observation and mechanical property testing were cut from the central part of the billets. The microstructure of the Ti samples was observed by transmission electron microcopy (TEM, FEI Tecnai G2 T20, Hillsboro, OR, USA). The samples were machined parallel to the longitudinal axis and mechanically thinned to ~60 μm, and finally twin jet polished with a solution of 6% perchloric acid and 94% ethanol. TEM images and the corresponding patterns of selected area electron diffraction (SAED) were taken by using an FEI Tecnai G2 electron microscope. The operating voltage was 200 KV.

Tensile samples were machined from the central regions of the processed billet parallel to the pressing direction, with a gauge length of 6 mm. The gauge width and thickness were 2 mm and 2 mm, respectively. The displacement rate of the tensile tests was 1 mm min^{-1} and the temperature was 25 °C. At least three samples for each state were tested and the final tensile curve for each state was the closest one to the average of the tests.

3. Results

3.1. Microstructure Evolution of Pure Titanium during RD-ECAP

The microstructure of the as-received and RD-ECAP processed titanium samples are shown in Figure 2. The initial grain size of the unprocessed titanium sample was about ~10 μm. After one

and two passes of RD-ECAP, the grains were still coarse, and high density of twins could be seen in the interior of grains, as shown in Figure 2b. There were no distinct dislocation cells or sub-grain boundaries observed, suggesting that the strain imposed after two passes was not sufficient to provide a significant grain refinement. After three passes, dislocation cells were detected and some sub-grains began to form, as shown in Figure 2c. More dislocation tangled in the grains rather than twins. The grain size was about 800 nm after three passes of ECAP. The rings in the diffraction patterns were not continual, indicating a small quantity of high-angle grain boundaries. After four passes, the grains were further refined and the grain size was only ~500 nm. The rings in the diffraction patterns were more intensive than that in Figure 2c, indicating the formation of more sub-grains. A fairly high density of dislocations could be observed in the grains, but twinning was hardly detected.

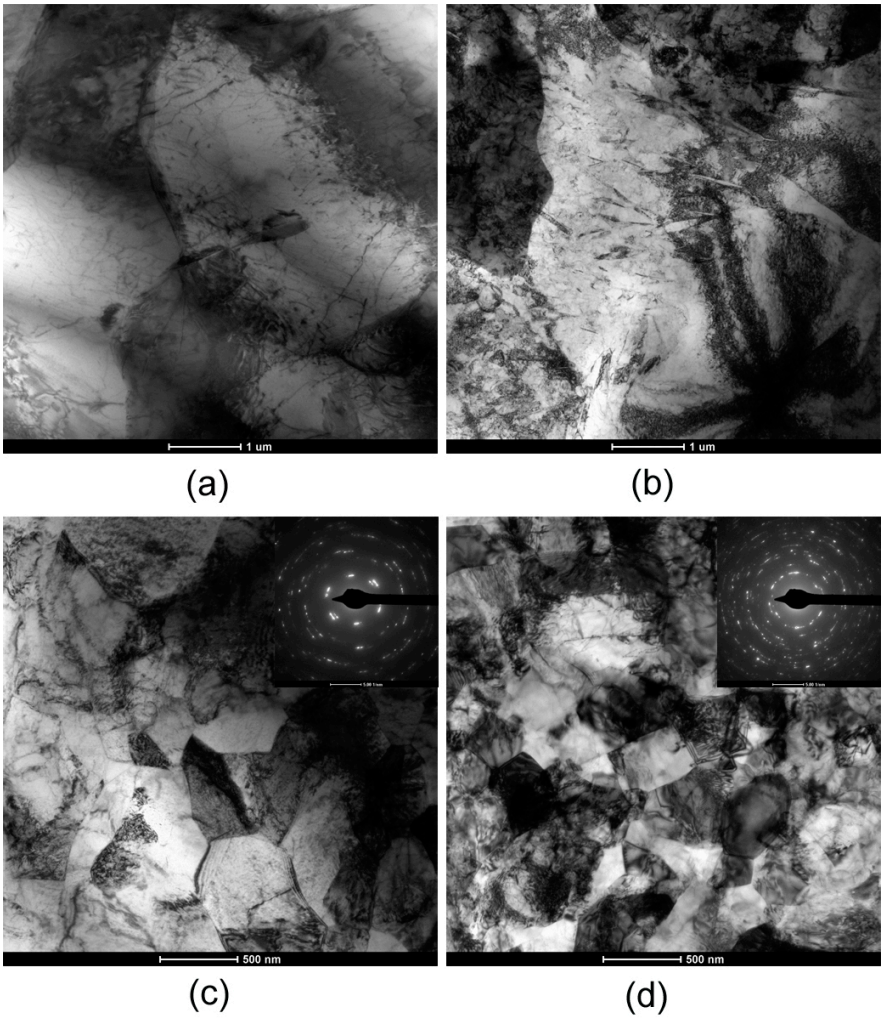

Figure 2. TEM micrographs and SAED patterns of pure Ti processed by RD-ECAP for: (**a**) zero passes; (**b**) two passes; (**c**) three passes; (**d**) four passes.

Figure 3 shows the TEM microstructure of the titanium sample after one pass of RD-ECAP. An important characteristic of the microstructure is that narrow and wide bands were alternately observed. The width of the bands varied from 300 nm to 1 μm. In order to clarify the structure of the bands, SAED patterns of region b (the wide band), region c (the narrow band), and region d (the junction zone of two adjacent bands) were taken with the $[2\bar{1}\bar{1}0]$ zone axis. It is observed that the wide bands were matrix, and the narrow bands were twinned regions. An analysis inferred that the twins were of $\{10\bar{1}2\}$ type. The twins exhibited a bending and distort configuration due to deformation.

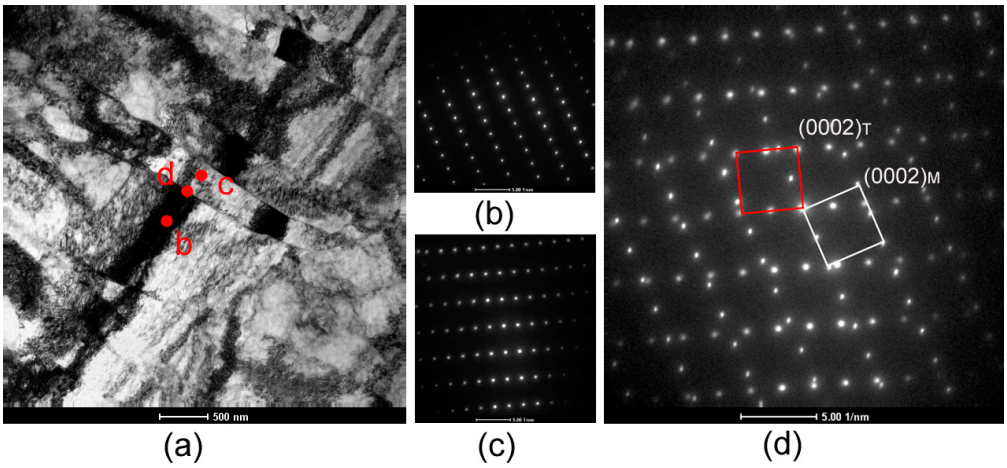

Figure 3. TEM microstructure of CP Ti processed by RD-ECAP for one pass showing $\{10\bar{1}2\}$ twinning: (**a**) micrographs of bands configuration; (**b**–**d**) the corresponding selected area electron diffractions of the regions indicated in (**a**). The zone axis is $[2\bar{1}\bar{1}0]$.

After two passes of RD-ECAP, elongated parallel bands in another configuration were observed in some region, as shown in Figure 4. The partial enlarged detail in Figure 4b shows that the width of the bands was ~500 nm. The dislocation density in these bands was not very high. SAED patterns of several adjacent bands demonstrated that region d and region f had the same patterns, while the region e between d and f showed mirror spots with respect to a plane. The SAED pattern of region c (the connected domain of d and e) indicated that the two adjacent bands constituted a $\{10\bar{1}1\}$ twin structure, as depicted in Figure 4c.

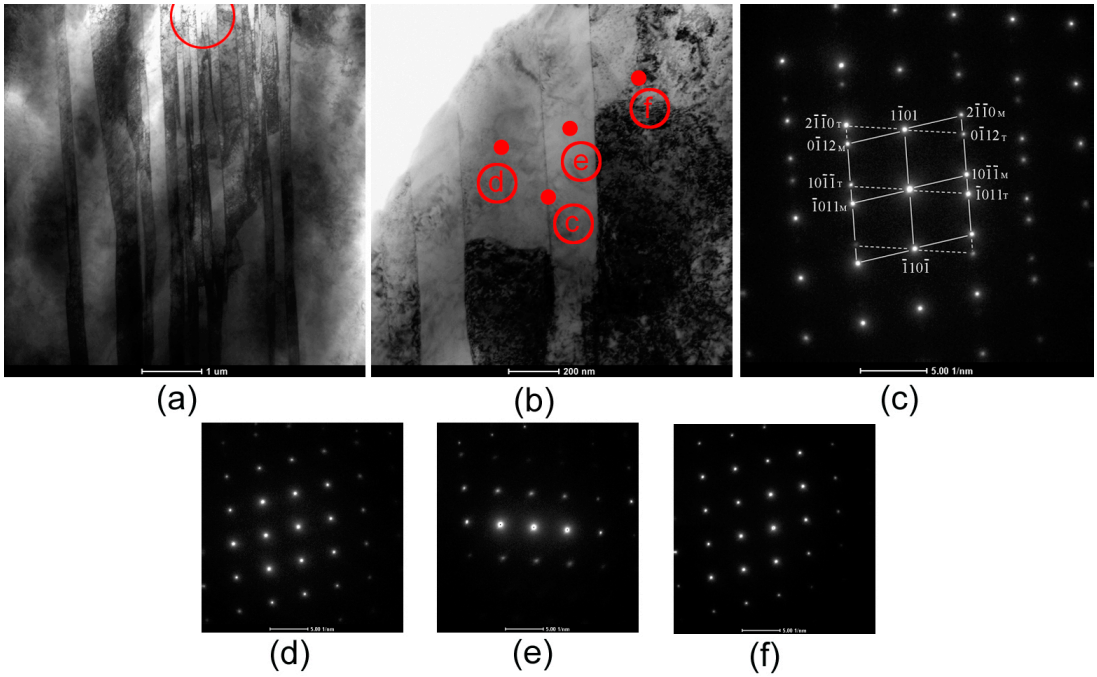

Figure 4. TEM microstructure of CP Ti processed by RD-ECAP for two passes showing $\{10\bar{1}1\}$ twinning: (**a**) micrographs of elongated parallel bands; (**b**) partial enlarged detail of the inner region of the red circle in (**a**); (**c**–**f**) the corresponding selected area electron diffractions of the regions indicated in (**b**). The zone axis is $[01\bar{1}1]$.

Figure 5 presents the microstructure after three passes of RD-ECAP. The dislocation density was fairly high and only a little spear-shaped twinning was detected in pure titanium after three passes of RD-ECAP. The total quantity of twinning in thrice-passed samples was rather low in contrast to the samples after one and two passes. The SAED pattern suggested that the twins were identified as $\{10\bar{1}1\}$ type.

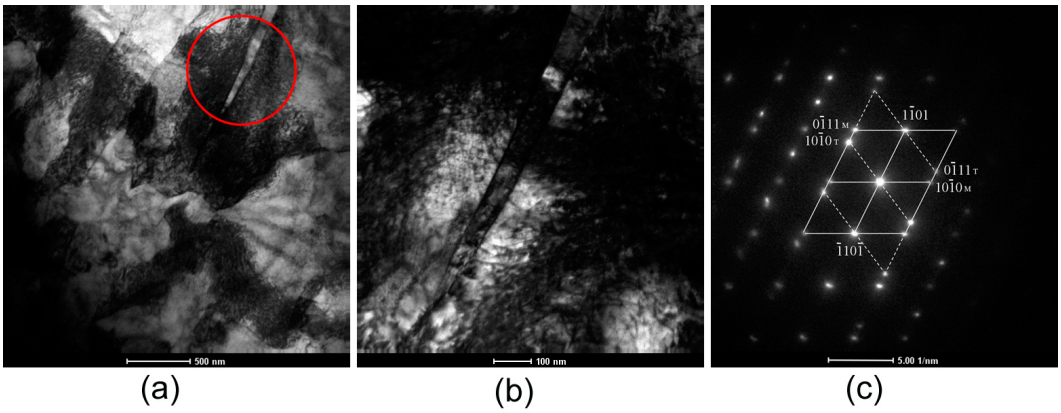

Figure 5. TEM microstructure of CP Ti processed by RD-ECAP for three passes showing $\{10\bar{1}1\}$ twinning: (**a**) micrographs of spear-shaped twinning; (**b**) partial enlarged detail of the inner region of the red circle in (**a**); (**c**) the corresponding selected area electron diffraction for the $[1\bar{2}1\bar{3}]$ zone axis.

3.2. Mechanical Properties after RD-ECAP Processing

Figure 6 shows the tensile curves of the unprocessed sample and the samples processed by one to four passes of RD-ECAP. It is distinct that the as-received sample exhibited a low ultimate strength and a reasonable elongation. The ultimate tensile strength was increased by the RD-ECAP processing, but the elongation was reduced. As the pass number increased, there was an enhancement of ultimate tensile strength, while the fracture elongation of the as-received sample was ~48% and decreased to ~29% after RD-ECAP processing. The ultimate tensile strength of the as-received state was ~450 MPa, which was increased to ~627 MPa after four passes of RD-ECAP, making an increase of 39%.

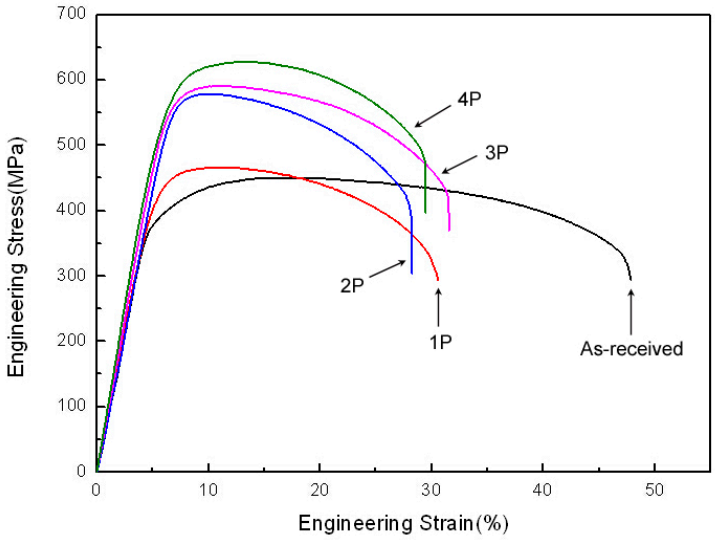

Figure 6. Tensile properties of the as-received titanium sample and specimens processed by RD-ECAP for one to four passes.

4. Discussion

4.1. Microstructure Characteristics and Deformation Behavior

The microstructure evolution of pure titanium during RD-ECAP for four passes showed that the plastic deformation was comprised of twinning and dislocation slip. As investigated above, the deformation during the first two passes was accommodated mainly by twinning. This is due to the limited slip systems of titanium as a hexagonal close-packed (hcp) metal. When the number of passes increased, the frequency of twinning decreased, and accordingly the dislocation density was increased. As a consequence, it is possible that twinning played an important role in the deformation during RD-ECAP processing by activating slip systems through converting orientations. Dislocation slip was the main deformation mechanism during the third and fourth passes.

Regarding the twinning mode of titanium during the first pass of ECAP processing, Kim et al. [18] demonstrated that the first pass of ECAP above 250 °C was dominated by $\{10\bar{1}1\}$ twinning and there was not any other twinning mode observed. Chen et al. [20] detected $\{10\bar{1}1\}$ twinning as the main twinning mode in the first pass of ECAP at 450 °C, with a small amount of $\{10\bar{1}2\}$ twinning. Meredith and Khan [26] also found that $\{10\bar{1}1\}$ twinning was the main contributor to deformation in pure titanium processed by ECAP for one pass at 275 °C. Zhao et al. [21] observed $\{10\bar{1}1\}$ twinning in the first pass of ECAP performed at room temperature. In contrast, only $\{10\bar{1}2\}$ twinning in titanium samples by the first pass of ECAP at room temperature was reported by Zhang et al. [22]. The above results demonstrate that the activation of twinning modes after one pass of ECAP related strongly to many internal and external conditions, for example, grain size of the initial material, pressing temperature, pressing speed, and so on, as listed in Table 1.

In the present study, we only detected the formation of $\{10\bar{1}2\}$ twins rather than $\{10\bar{1}1\}$ twins in pure titanium processed by one pass of RD-ECAP at 420 °C. This may be on account of the relatively small grain size of initial material in the present study. Kim et al. [27] found that the deformation mode in pure titanium during ECAP was strongly dependent on the initial grain size. Moreover, another possible influencing factor may be the relatively low pressing speed employed in this work, which is connected with the strain rate. Kim et al. [27] found in the same research that a higher pressing speed during ECAP promoted the formation of $\{10\bar{1}1\}$ twinning.

Table 1. List of different twinning modes of CP Ti after one pass of ECAP.

Grain Size (μm)	Pressing Temperature (°C)	Pressing Speed (mm/s)	Twinning	Reference
~30	350	2	$\{10\bar{1}1\}$	Kim et al. [28]
~30	250–450	2	$\{10\bar{1}1\}$	Kim et al. [18]
~28	RT	0.5	$\{10\bar{1}1\}$	Zhao et al. [21]
~40–120	390–400	8	$\{10\bar{1}1\}$	Fan et al. [29]
-	450	2	$\{10\bar{1}1\}$	Li et al. [19]
~22	450	-	$\{10\bar{1}1\}\{10\bar{1}2\}$	Chen et al. [20]
~200	RT	-	$\{10\bar{1}1\}\{11\bar{2}1\}\{10\bar{1}2\}\{11\bar{2}2\}$	Chen et al. [23]
~30	275	1	$\{10\bar{1}1\}$	Meredith et al. [26]
~10	RT	0.05	$\{10\bar{1}2\}$	Zhang et al. [22]
~10	420	0.1	$\{10\bar{1}2\}$	Present Study

After two passes of RD-ECAP, a great quantity of $\{10\bar{1}1\}$ twins were detected, as shown in Figure 4, and the density of dislocations in these twin bands was not very high. Moreover, the microstructure depicted in Figure 2b revealed that the density of dislocation was not high enough to constitute dislocation cells and sub-grain boundaries for grain refinement. It seems that only a small part of slip systems was motivated, and the predominant deformation mechanism was still twinning during the second pass of RD-ECAP. Hence, the critical resolved shear stress (CRSS) for twinning at the second pass was still lower than that for dislocation slip. However, this is not in accordance with the earlier results reported by Shin et al. [30], that plastic deformation was predominantly accommodated by dislocation slip during the second pass of ECAP. This difference may be due to the microstructure

discrepancy after the first pass, for instance, the refinement of grain size, the formation of texture, and the twinning mode. Shin et al. [30] pointed out that the deformation modes during the second pass strongly hinged on the processing route. The deformation manner in the RD-ECAP is different from the routes A, B, or C of conventional ECAP. The alternated front and rear parts of samples in RD-ECAP make the deformation quite distinct from route A, in which the pressing direction of each pass is the same. Thus, the microstructure characterization during the second pass of RD-ECAP may be related to the special deformation path.

After three passes of RD-ECAP, the density of dislocations increased and there was a significant refinement of grains. Meanwhile, only a small fraction of $\{10\bar{1}1\}$ twins were detected. It is evident that the main plastic deformation was dislocation slip during the third pass of RD-ECAP processing. This means that the CRSS for twinning exceeded that for dislocation slip during the third RD-ECAP pass. As the decrease of grain size, the CRSS for both twinning and slip increased, however, it is probable that the increase rate of the twinning stress was larger than of the dislocation slip.

During the fourth pass of RD-ECAP, the dislocation density was further increased and the primary deformation mechanism was dislocation slip in place of twinning. Grains of titanium were further refined by the generation of sub-grains.

Overall, the sequence of the main deformation structure in pure titanium subjected to RD-ECAP at 420 °C in the present study can be described as: $\{10\bar{1}2\}$ twinning in the first pass, $\{10\bar{1}1\}$ twinning in the second pass, and dislocation slip in the third and fourth passes.

4.2. Mechanical Properties

As illustrated in Figure 2b, there was not a remarkable refinement of grain size after two passes, so the strengthening after one and two passes was mainly attributed to twinning and dislocation generation. After three and four passes, the grains were refined and the strengthening primarily resulted from finer grain size and high-density dislocation. It is advantageous to notice that the ultimate tensile strength of ~627 MPa after RD-ECAP for four passes at 420 °C is an improvement over the reported ~540 MPa processed for seven passes by ECAP at 450 °C–500 °C [31]. Moreover, it is comparable with the ultimate tensile strength of ~645 MPa achieved after 10 passes of ECAP at 400 °C–450 °C [24]. Therefore, it is confirmed from the present results that RD-ECAP processing has the potential of processing high strength UFG pure titanium conveniently and efficiently.

5. Conclusions

(1) Pure titanium of grade 2 was successfully processed by RD-ECAP up to four passes at 420 °C. There was no cracking on the sample surface.

(2) During the first and second passes of RD-ECAP, plastic deformation was accommodated mainly by twins, while the predominant deformation mechanism was dislocation slip during the third and fourth passes. $\{10\bar{1}2\}$ twins were detected in the first pass, and $\{10\bar{1}1\}$ twins occurred in the second pass of RD-ECAP.

(3) There was an increase of ~39% in ultimate tensile strength after processing by RD-ECAP for four passes. The ultimate tensile strength increased from 450 MPa of the as-received condition to 627 MPa after four passes of RD-ECAP, while the elongation decreased from ~48% to ~29%.

Acknowledgments: The study was supported by the Fundamental Research Funds for the Central Universities (grant number HHU2016B10314), the Research Innovation Program for Graduate students of Jiangsu Province of China (grant number SJZZ16_0092), Six Major Talent Peaks Project of Jiangsu Province of China (grant number 2014-XCL-023), the Public Service Platform and Science & Technology Support Program in the industrial field of Suqian City of China (grant number M201614 & H201615).

Author Contributions: Aibin Ma and Jinghua Jiang conceived and designed the experiments; Yanxia Gu and Huiyun Li performed the experiments; Yanxia Gu and Yuchun Yuan analyzed the data; Yanxia Gu contributed reagents/materials/analysis tools; Yanxia Gu wrote the paper.

Conflicts of Interest: The authors declare no conflict of interest.

References

1. Valiev, R.Z.; Langdon, T.G. Principles of equal-channel angular pressing as a processing tool for grain refinement. *Prog. Mater. Sci.* **2006**, *51*, 881–981. [CrossRef]
2. Valiev, R.Z.; Estrin, Y.; Horita, Z.; Langdon, T.G.; Zehetbauer, M.J.; Zhu, Y. Producing bulk ultrafine-grained materials by severe plastic deformation: Ten years later. *JOM* **2016**, *68*, 1216–1226. [CrossRef]
3. Valiev, R.Z.; Islamgaliev, R.K.; Alexandrov, I.V. Bulk nanostructured materials from severe plastic deformation. *Prog. Mater. Sci.* **2000**, *45*, 103–189. [CrossRef]
4. Nishida, Y.; Arima, H.; Kim, J.; Ando, T. Rotary-die equal-channel angular pressing of an al-7mass%si-0.35mass%mg alloy. *Scr. Mater.* **2001**, *45*, 261–266. [CrossRef]
5. Ma, A.B.; Nishida, Y.; Suzuki, K.; Shigematsu, I.; Saito, N. Characteristics of plastic deformation by rotary-die equal-channel angular pressing. *Scr. Mater.* **2005**, *52*, 433–437. [CrossRef]
6. Yoon, S.C.; Seo, M.H.; Krishnaiah, A.; Kim, H.S. Finite element analysis of rotary-die equal channel angular pressing. *Mater. Sci. Eng. A* **2008**, *490*, 289–292. [CrossRef]
7. Elias, C.N.; Meyers, M.A.; Valiev, R.Z.; Monteiro, S.N. Ultrafine grained titanium for biomedical applications: An overview of performance. *J. Mater. Res. Technol.* **2013**, *2*, 340–350. [CrossRef]
8. Xu, S.; Toth, L.S.; Schuman, C.; Lecomte, J.S.; Barnett, M.R. Dislocation mediated variant selection for secondary twinning in compression of pure titanium. *Acta Mater.* **2017**, *124*, 59–70. [CrossRef]
9. Chun, Y.B.; Yu, S.H.; Semiatin, S.L.; Hwang, S.K. Effect of deformation twinning on microstructure and texture evolution during cold rolling of cp-titanium. *Mater. Sci. Eng. A* **2005**, *398*, 209–219. [CrossRef]
10. Li, X.; Duan, Y.L.; Xu, G.F.; Peng, X.Y.; Dai, C.; Zhang, L.G.; Li, Z. Ebsd characterization of twinning in cold-rolled cp-ti. *Mater. Charact.* **2013**, *84*, 41–47. [CrossRef]
11. Tirry, W.; Bouvier, S.; Benmhenni, N.; Hammami, W.; Habraken, A.M.; Coghe, F.; Schryvers, D.; Rabet, L. Twinning in pure ti subjected to monotonic simple shear deformation. *Mater. Charact.* **2012**, *72*, 24–36. [CrossRef]
12. Won, J.W.; Kim, D.; Hong, S.G.; Lee, C.S. Anisotropy in twinning characteristics and texture evolution of rolling textured high purity alpha phase titanium. *J. Alloys Compd.* **2016**, *683*, 92–99. [CrossRef]
13. Xu, F.; Zhang, X.; Ni, H.; Liu, Q. Deformation twinning in pure ti during dynamic plastic deformation. *Mater. Sci. Eng. A* **2012**, *541*, 190–195. [CrossRef]
14. Jin, S.; Marthinsen, K.; Li, Y. Formation of {1121} twin boundaries in titanium by kinking mechanism through accumulative dislocation slip. *Acta Mater.* **2016**, *120*, 403–414. [CrossRef]
15. Hong, D.H.; Hwang, S.K. Microstructural refinement of cp-ti by cryogenic channel-die compression involving mechanical twinning. *Mater. Sci. Eng. A* **2012**, *555*, 106–116. [CrossRef]
16. Wang, T.; Li, B.; Li, M.; Li, Y.; Wang, Z.; Nie, Z. Effects of strain rates on deformation twinning behavior in α-titanium. *Mater. Charact.* **2015**, *106*, 218–225. [CrossRef]
17. Hama, T.; Nagao, H.; Kobuki, A.; Fujimoto, H.; Takuda, H. Work-hardening and twinning behaviors in a commercially pure titanium sheet under various loading paths. *Mater. Sci. Eng. A* **2015**, *620*, 390–398. [CrossRef]
18. Kim, I.; Kim, J.; Shin, D.H.; Lee, C.S.; Hwang, S.K. Effects of equal channel angular pressing temperature on deformation structures of pure ti. *Mater. Sci. Eng. A* **2003**, *342*, 302–310. [CrossRef]
19. Li, Y.J.; Chen, Y.J.; Walmsley, J.C.; Mathinsen, R.H.; Dumoulin, S.; Roven, H.J. Faceted interfacial structure of $\{10\bar{1}1\}$ twins in ti formed during equal channel angular pressing. *Scr. Mater.* **2010**, *62*, 443–446. [CrossRef]
20. Chen, Y.J.; Li, Y.J.; Walmsley, J.C.; Dumoulin, S.; Gireesh, S.S.; Armada, S.; Skaret, P.C.; Roven, H.J. Quantitative analysis of grain refinement in titanium during equal channel angular pressing. *Scr. Mater.* **2011**, *64*, 904–907. [CrossRef]
21. Zhao, X.; Fu, W.; Yang, X.; Langdon, T.G. Microstructure and properties of pure titanium processed by equal-channel angular pressing at room temperature. *Scr. Mater.* **2008**, *59*, 542–545. [CrossRef]
22. Zhang, Y.; Figueiredo, R.B.; Alhajeri, S.N.; Wang, J.T.; Gao, N.; Langdon, T.G. Structure and mechanical properties of commercial purity titanium processed by ecap at room temperature. *Mater. Sci. Eng. A* **2011**, *528*, 7708–7714. [CrossRef]
23. Chen, Y.J.; Li, Y.J.; Xu, X.J.; Hjelen, J.; Roven, H.J. Novel deformation structures of pure titanium induced by room temperature equal channel angular pressing. *Mater. Lett.* **2014**, *117*, 195–198. [CrossRef]

24. Stolyarov, V.V.; Zeipper, L.; Mingler, B.; Zehetbauer, M. Influence of post-deformation on cp-ti processed by equal channel angular pressing. *Mater. Sci. Eng. A* **2008**, *476*, 98–105. [CrossRef]
25. Valiev, R.Z.; Semenova, I.P.; Jakushina, E.; Latysh, V.V.; Rack, H.J.; Lowe, T.C.; Petruželka, J.; Dluhoš, L.; Hrušák, D.; Sochová, J. Nanostructured spd processed titanium for medical implants. *Mater. Sci. Forum* **2008**, *584–586*, 49–54. [CrossRef]
26. Meredith, C.S.; Khan, A.S. The microstructural evolution and thermo-mechanical behavior of ufg ti processed via equal channel angular pressing. *J. Mater. Process. Technol.* **2015**, *219*, 257–270. [CrossRef]
27. Kim, I.; Kim, J.; Shin, D.H.; Park, K.T. Effects of grain size and pressing speed on the deformation mode of commercially pure ti during equal channel angular pressing. *Metall. Mater. Trans. A* **2003**, *34A*, 1555–1558. [CrossRef]
28. Kim, I.; Jeong, W.S.; Kim, J.; Park, K.T.; Shin, D.H. Deformation structures of pure ti produced by equal channel angular pressing. *Scr. Mater.* **2001**, *45*, 575–581. [CrossRef]
29. Fan, Z.; Jiang, H.; Sun, X.; Song, J.; Zhang, X.; Xie, C. Microstructures and mechanical deformation behaviors of ultrafine-grained commercial pure (grade 3) ti processed by two-step severe plastic deformation. *Mater. Sci. Eng. A* **2009**, *527*, 45–51. [CrossRef]
30. Shin, D.H.; Kim, I.; Kim, J.; Kim, Y.S.; Semiatin, S.L. Microstructure development during equal-channel angular pressing of titanium. *Acta Mater.* **2003**, *51*, 983–996. [CrossRef]
31. Stolyarov, V.V.; Zhu, Y.T.; Lowe, T.C.; Islamgaliev, R.K.; Valiev, R.Z. A two step spd processing of ultrafine-grained titanium. *Nanostruct. Mater.* **1999**, *11*, 947–954. [CrossRef]